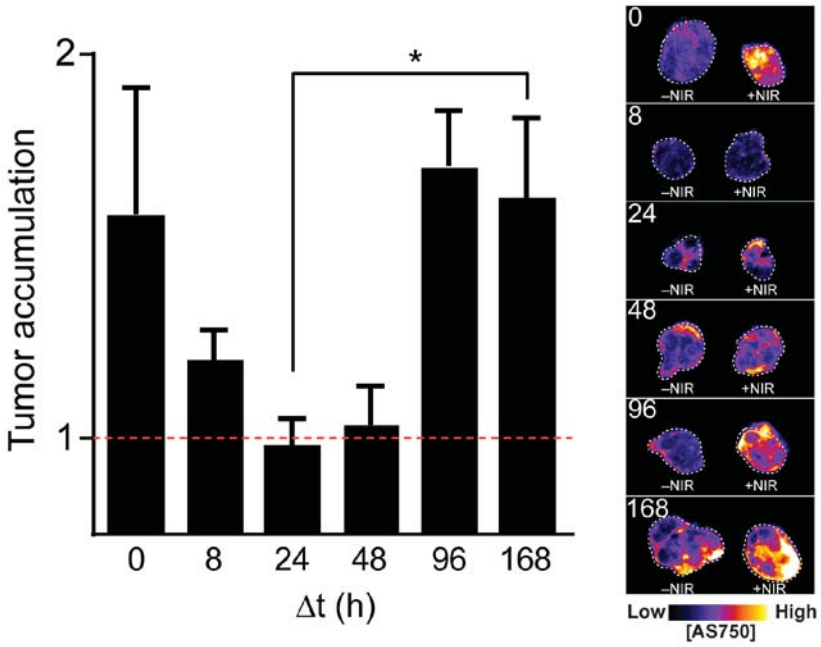


**Supplementary Figure 1.** Tumor accumulation of AS750 after PEG-NR heat exposure with varying delta T. Tumor transport (ratio of AS750 for cohorts of heated versus unheated tumors) and two representative images of tumors that were explanted after PEG-NR heating with delta T values ranging between 0 h to 1 week, and assayed by IVIS for AS750 transport. (n = 4-9 per group from two independent experiments, *P<0.05, one-way ANOVA and Tukey's post-tests.) Error bars, SE.

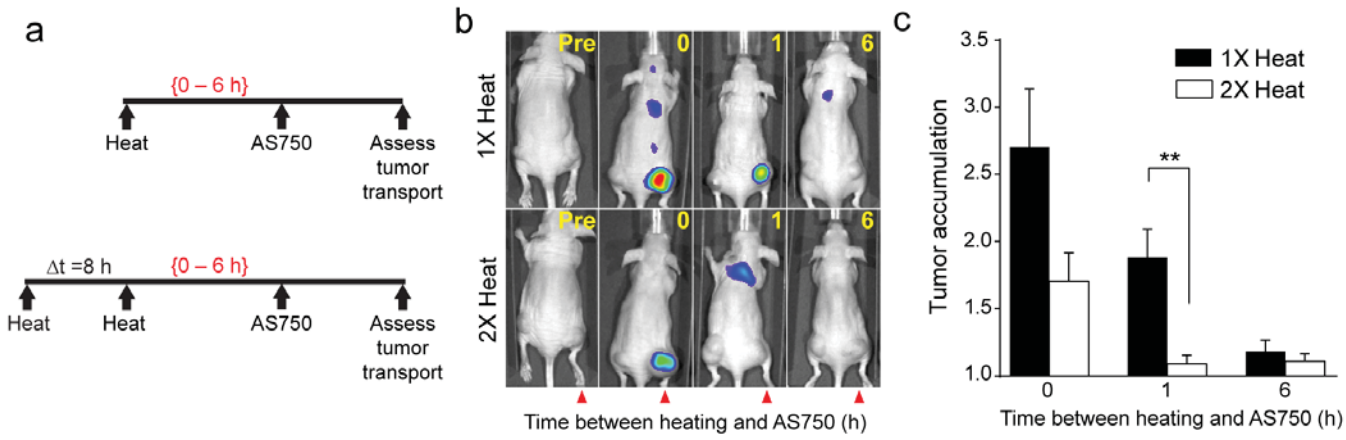


**Supplementary Figure 2.** Diminished window of tumor transport after re-exposure to PEG-NR heating. (a) Experimental time course includes an initial exposure to PEG-NR heating (heat), an interval delta T of 8 h, re-exposure to PEG-NR heating (heat, 2X group), and AS750 administration offset from the final heating by 0, 1, or 6 h. Tumor accumulation is quantified via in vivo fluorescence imaging. (b) Representative in vivo fluorescence images demonstrating shortened window of tumor transport after re-exposure to PEG-NR heating. Red arrows indicate heated tumors. (c) Tumor transport (ratio of AS750 in heated versus unheated tumors) for each cohort with the indicated offset in AS750 administration after re-exposure to heating. (n = 8 per group, **P<0.01, unpaired t-test, two-tailed.) Error bars, SE.

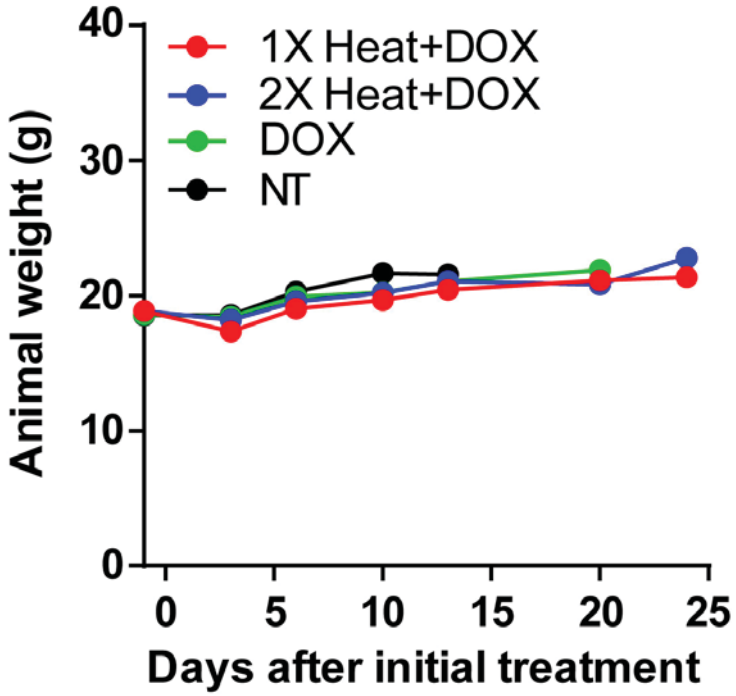


**Supplementary Figure 3.** Animal weights during PEG-NR and doxorubicin liposome therapeutic trial. Weights remained consistent among treatment groups during the trial period. (n = 8-9 per group) Error bars, SE.

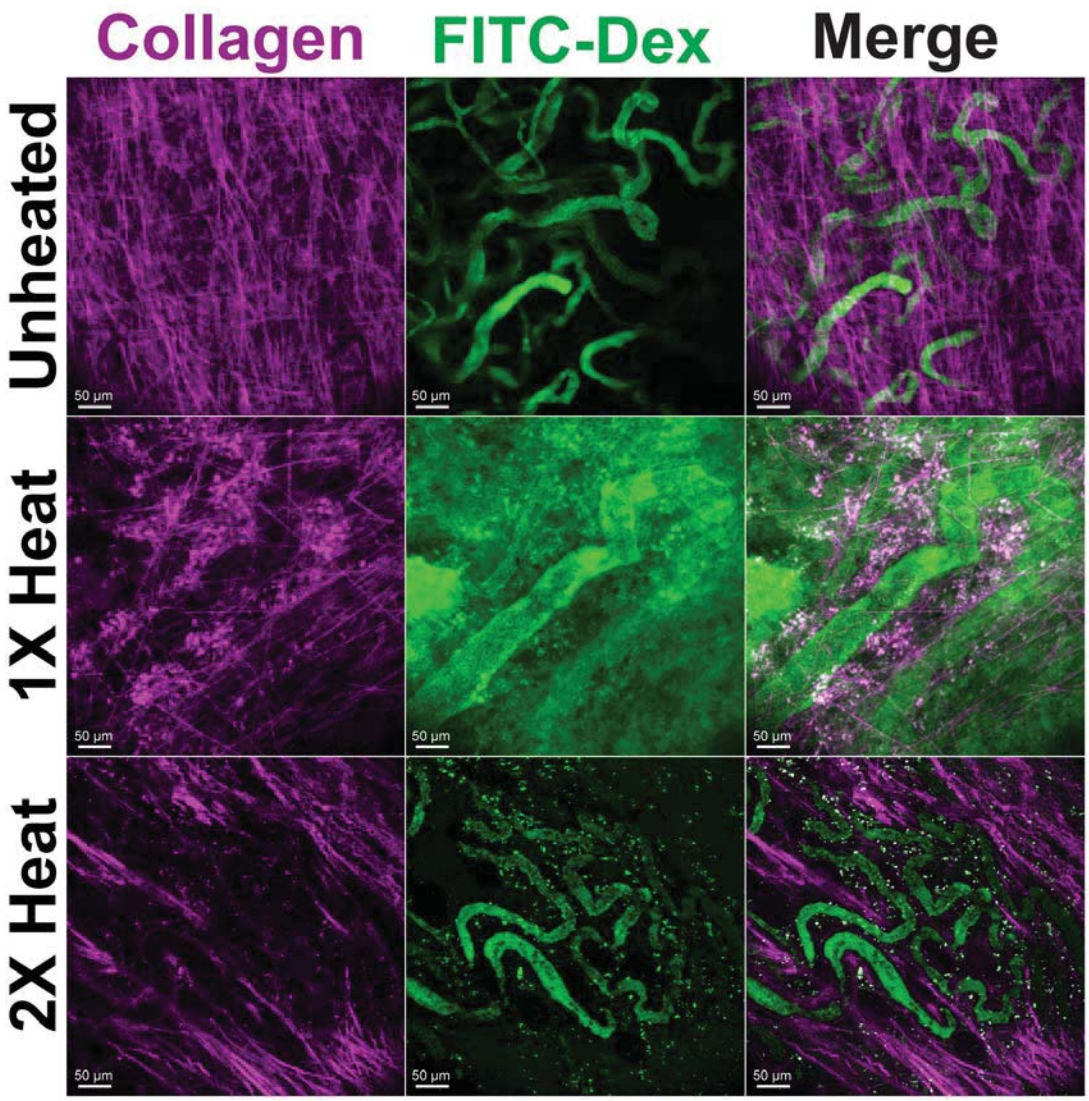


**Supplementary Figure 4.** Transvascular transport in tumors after single exposure and re-exposure to PEG-NR heating. Unheated and re-exposure (2X heat) tumor vessels display intravascular retention of 70 kDa FITC-Dextran, while a greater degree of extravasation of FITC-Dextran was observed during single exposures (1X heat) to PEG-NR heating. Collagen fibers (magenta) delineate the tumor interstitium and PEG-NRs appear in a punctate perivascular pattern in both channels. (n = 15-31 z-stacks from n = 3-7 animals per treatment group) Scale bar: 50 µm

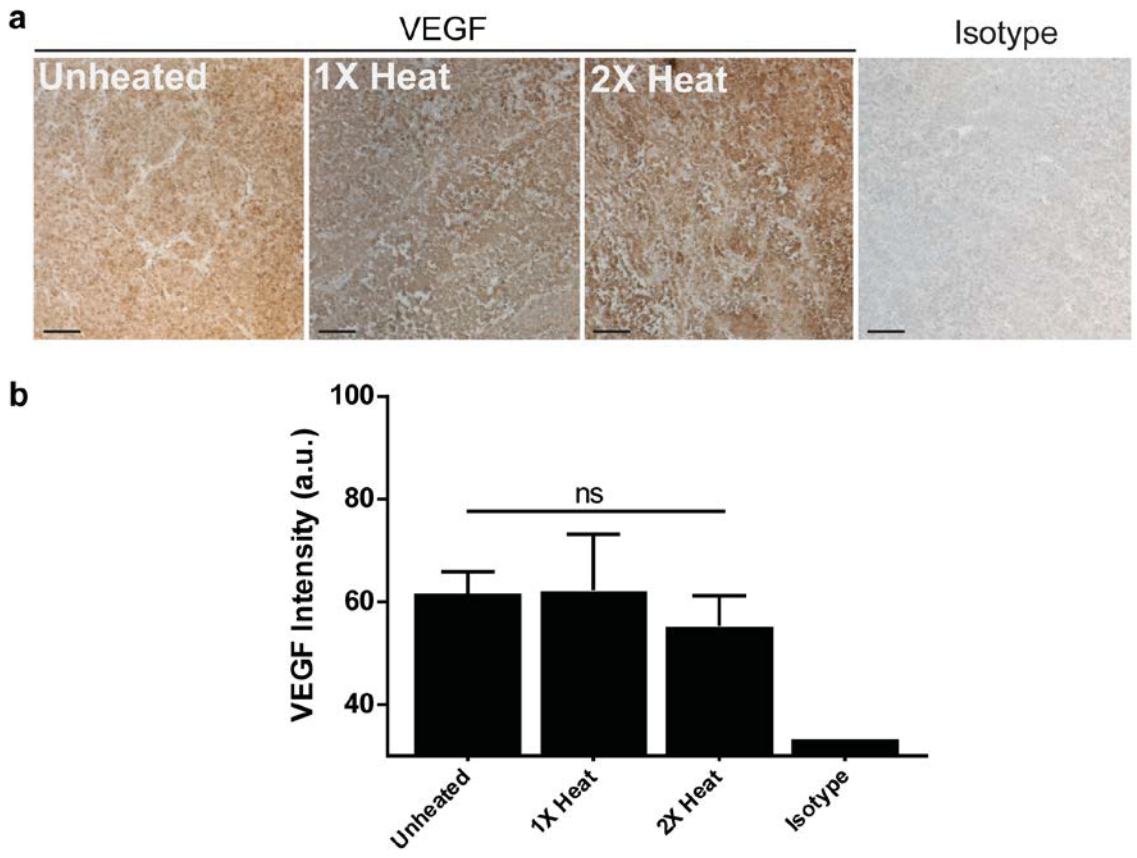


**Supplementary Figure 5.** Vascular endothelial growth factor (VEGF) expression in PEG-NR heated tumors. (a) Representative images illustrating VEGF expression in tumors either unheated or receiving a single exposure or re-exposure to PEG-NR heating. (b) Mean immunohistochemical staining intensity of large scan images of the tumor cross-sectional area. No significant differences were observed in VEGF intensity between the unheated, single, and repeat PEG-NR heated groups. (n = 4-6 tumors per group) Error bars, SE. Scale bar: 100 μm

a

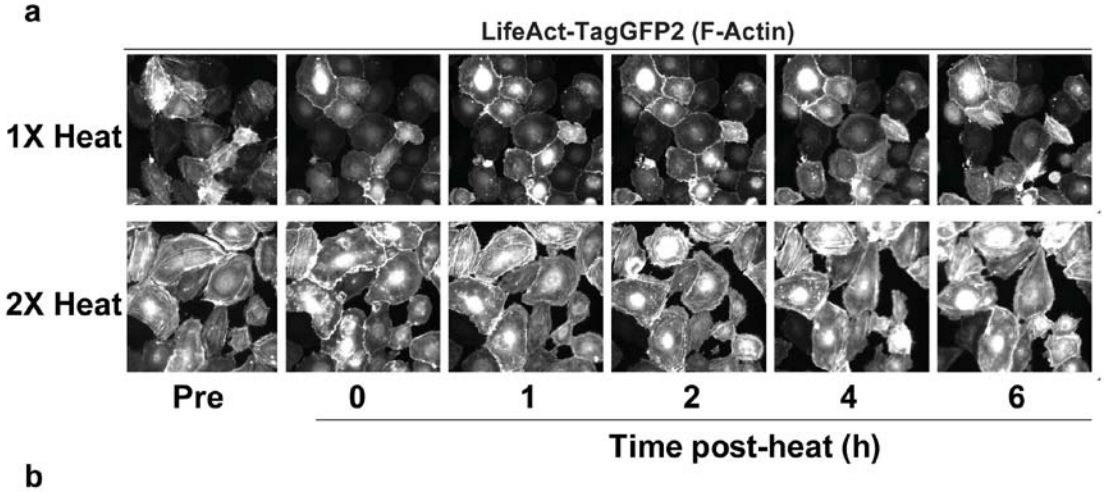


b

| Condition | Time Post heat (h) | Fields Examined | Total Cells | Filament-Positive Cells (Mean ± SD) | Total Cells (Mean ± SD) | % Filament-Positive (Mean ± SD) |
|---|---|---|---|---|---|---|
| 1X | Pre | 6 | 1072 | 111.83 ± 15.61 | 178.67 ± 21.65 | 62.92 ± 8.14 |
| | 0 | 6 | 1107 | 7.83 ± 6.18 | 184.50 ± 22.47 | 4.08 ± 3.12 |
| | 1 | 6 | 1213 | 6.00 ± 4.20 | 202.17 ± 10.93 | 2.97 ± 2.13 |
| | 2 | 6 | 1172 | 13.83 ± 8.06 | 195.33 ± 15.49 | 7.15 ± 4.45 |
| | 4 | 6 | 1123 | 42.67 ± 20.18 | 187.17 ± 13.32 | 22.95 ± 11.09 |
| | 6 | 6 | 1154 | 57.17 ± 40.18 | 192.33 ± 17.43 | 30.39 ± 21.81 |
| 2X | Pre | 8 | 1117 | 101.25 ± 21.40 | 139.63 ± 13.21 | 72.62 ± 13.92 |
| | 0 | 8 | 1161 | 24.25 ± 8.48 | 145.13 ± 16.31 | 16.95 ± 6.22 |
| | 1 | 8 | 1150 | 90.88 ± 14.02 | 143.75 ± 13.71 | 63.61 ± 10.65 |
| | 2 | 8 | 1127 | 106.13 ± 10.86 | 140.88 ± 15.67 | 75.87 ± 9.08 |
| | 4 | 8 | 1099 | 99.75 ± 16.13 | 137.38 ± 12.66 | 72.38 ± 8.27 |
| | 6 | 8 | 1088 | 87.00 ± 12.46 | 136.00 ± 14.79 | 64.29 ± 9.22 |

**Supplementary Figure 6.** Endothelial cell F-Actin dynamics during heat exposure and recovery. (a) Representative images of endothelial F-actin filaments prior to heat exposure and 0 – 6 hours following heating for the single exposure (1X) and re-exposure (2X) groups. Loss of filament structure after heat exposure was observed in both single heat exposure and re-exposure groups, with more efficient recovery of filament structure in the re-exposure group. The same fields were imaged at each time point to enable measurements of actin dynamics in the same cells over time. (b) Quantification of endothelial cells and F-actin structure. A total of 13,583 individual cell measurements were scored for this analysis.

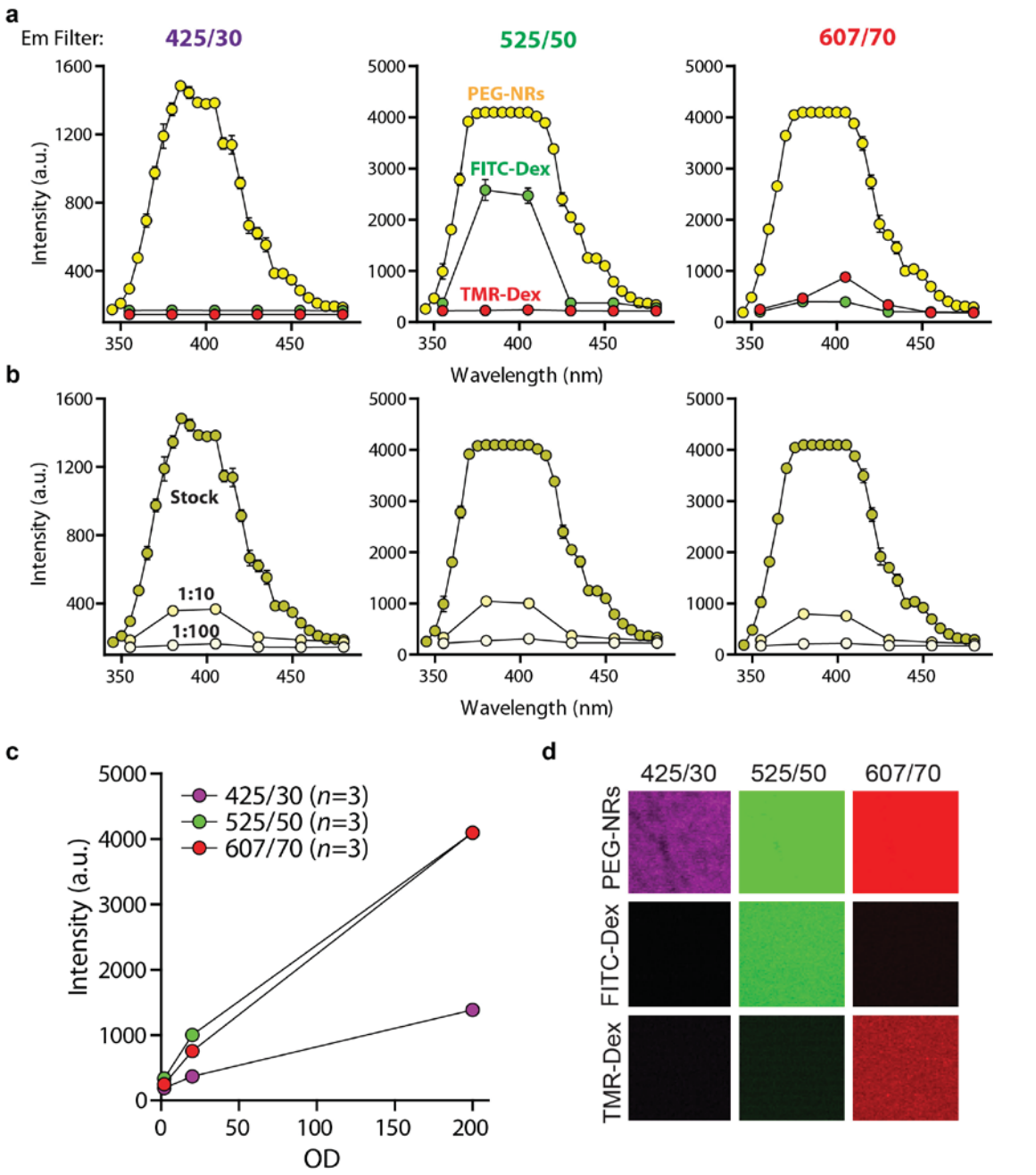


**Supplementary Figure 7.** Visualizing PEG-NRs in the tumor microenvironment using multiphoton microscopy. (**a**) Fluorescence/luminescence intensities of PEG-NRs (yellow), FITC-Dextran (green), and TMR-Dextran (red) with three separate emission filter channels (425/30, 525/50, and 607/70 nm). An intense signal with a peak at ~400nm was observed for PEG-NRs in all three channels. FITC-Dextran was detected with the 525/50 filter and TMR-Dextran with the 607/70 only. (**b**) Dose-dependent luminescence of PEG-NRs in each channel using 1:10 and 1:100 dilutions from stock PEG-NR concentration (OD: 200). (**c**) Plot of peak intensity versus PEG-NR optical density with each emission filter. (**d**) Images of PEG-NRs, FITC-Dextran, and TMR-Dextran acquired by multiphoton microscopy.

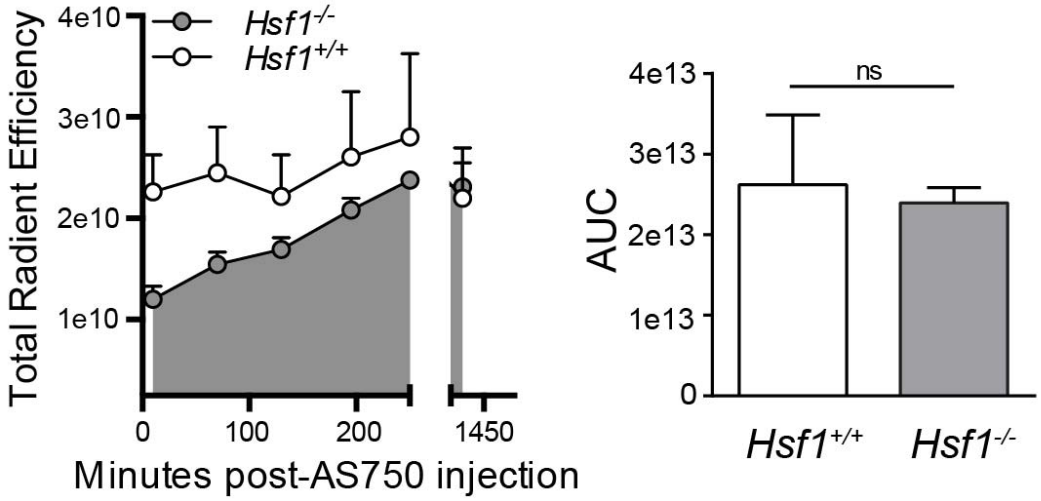


**Supplementary Figure 8.** Cargo accumulation in tumors with Hsf1+/+ and Hsf1-/- vasculature after single exposure to PEG-NR heating. Kinetics (a) and overall levels (b) of accumulation of AS750 up to 24 hours observed for both groups. Error bars, SE. (n = 3 per group)

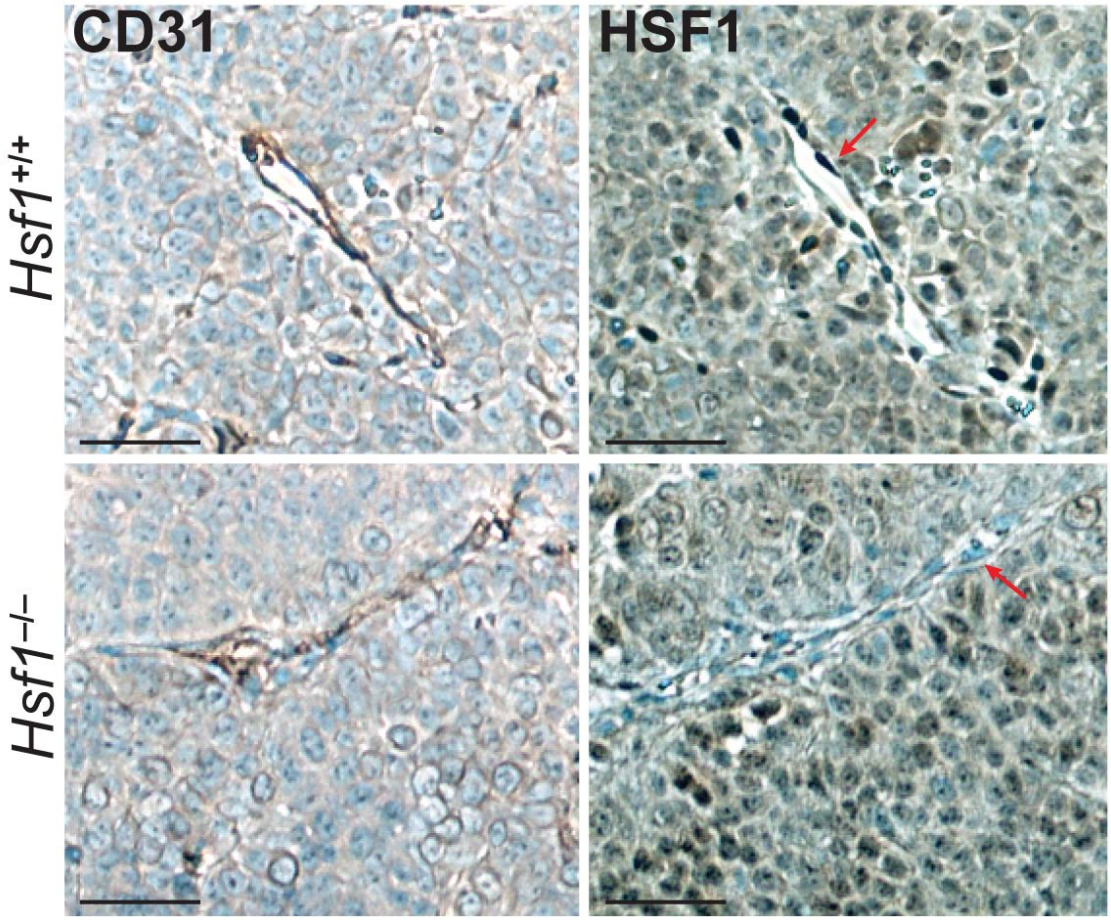


**Supplementary Figure 9.** HSF1 expression in tumor-associated vasculature following PEG-NR heating. Immunohistochemical staining of serial tissue sections for PECAM-1 (CD31) to label endothelial vessels and HSF1, counterstained with H&E. CD31-positive endothelium in *Hsf1*+/+ models displays a strong nuclear HSF1 staining pattern (red arrow), consistent with HSF1 activation and translocation to the nucleus with PEG-NR heating. CD31-positive endothelium in *Hsf1*-/- models displayed no observable HSF1 staining pattern (red arrow). In both models, positive HSF1 staining was detected in tumor parenchymal cells. Scale bar: 100 μm

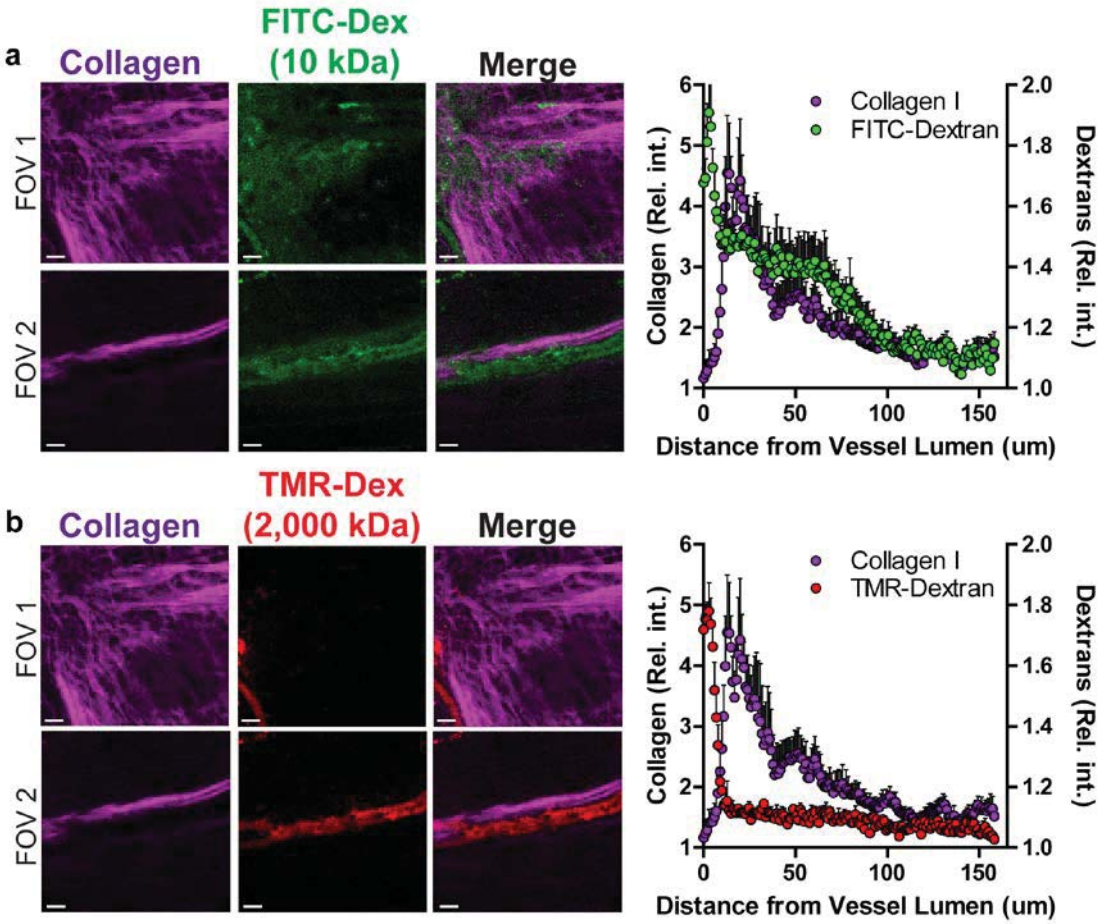


**Supplementary Figure 10.** Size-dependent macromolecular extravasation from the unheated vasculature. Intravenous co-administration of (a) 10 kDa FITC-Dextran and (b) 2,000 kDa TMR-Dextran revealed greater extravasation of the smaller molecular-weight compound, which appeared to become sequestered in regions with dense collagen fibers as shown by the correspondence in relative intensities on line histograms computed for collagen and FITC-Dextran. Larger molecular weight TMR-Dextran was retained within the vessel lumen in the same field of view, revealing the size-dependence of extravasation in our model. Scale bar: 50 μm